SCIENCE CHINA
Information Sciences

• RESEARCH PAPER •
Special Focus

May 2012 Vol. 55 No. 5: 1052–1061
doi: 10.1007/s11432-012-4556-0

Medical image segmentation using improved FCM

ZHANG XiaoFeng[1,2], ZHANG CaiMing[1,3,4*], TANG WenJing[1,2] & WEI ZhenWen[1]

[1] *School of Computer Science and Technology, Shandong University, Jinan* 250101*, China;*
[2] *School of Information and Electrical Engineering, Ludong University, Yantai* 264025*, China;*
[3] *School of Computer Science and Technology, Shandong University of Finance and Economics, Jinan* 250014*, China;*
[4] *Shandong Province Key Lab of Digital Media Technology, Jinan* 250014*, China*

Received October 21, 2011; accepted December 6, 2011; published online March 19, 2012

Abstract Image segmentation is one of the most important problems in medical image processing, and the existence of partial volume effect and other phenomena makes the problem much more complex. Fuzzy C-means, as an effective tool to deal with PVE, however, is faced with great challenges in efficiency. Aiming at this, this paper proposes one improved FCM algorithm based on the histogram of the given image, which will be denoted as HisFCM and divided into two phases. The first phase will retrieve several intervals on which to compute cluster centroids, and the second one will perform image segmentation based on improved FCM algorithm. Compared with FCM and other improved algorithms, HisFCM is of much higher efficiency with satisfying results. Experiments on medical images show that HisFCM can achieve good segmentation results in less than 0.1 second, and can satisfy real-time requirements of medical image processing.

Keywords FCM, histogram, image segmentation, medical image processing

Citation Zhang X F, Zhang C M, Tang W J, et al. Medical image segmentation using improved FCM. Sci China Inf Sci, 2012, 55: 1052–1061, doi: 10.1007/s11432-012-4556-0

1 Introduction

Image segmentation has become one common scientific issue and core technology in digital image processing [1,2]. In medical image processing, image segmentation plays a vital role in biomedical imaging applications such as the quantification of tissue volumes, diagnosis, localization of pathology, study of anatomical structure, treatment planning, partial volume correction of functional imaging data, and computer integrated surgery [3]. Currently, medical images suffer from three main problems: intensity inhomogeneity(IIH), noise and partial volume effect(PVE) [4,5]. Specifically, IIH appears as tissue intensity variation with locations, which may arise from radio frequency coils or acquisition sequences. PVE occurs where received signals contain a mixture of several tissues; thus it is difficult to assign one single class to the affected pixels. Therefore, conventional "hard" segmentation method cannot be applied to this phenomenon, because it restricts each pixel exclusively to one class. As a result, fuzzy classification has been extensively applied, since it can assign one pixel to several classes concurrently and can retain information as much as possible. Currently, there are two popular PVE models: fuzzy C-means(FCM) [6,7] and Gaussian distribution models [8,9]. In this paper, we will investigate FCM-based algorithms for medical image segmentation.

*Corresponding author (email: czhang@sdu.edu.cn)

As a typical unsupervised technique, FCM has been applied successfully in pattern recognition and data mining. However, when applied in medical image segmentation, FCM has two obvious defects: 1) since it only considers color information without any spatial one, FCM cannot achieve satisfying results; 2) FCM minimizes the objective function iteratively, which is of low efficiency and cannot fulfill real-time requirement of image processing. To solve these two problems, many researchers improved conventional FCM [7,10–12,14], and proposed such algorithms as FCM_S and EnFCM. In order to decrease the number of iterations, the objective function designed is much more complex, which will improve the running time of each iteration greatly. In some improved algorithms, it even takes more than one hour to accomplish one iteration [13], and so they are not suitable for medical image segmentation. Aiming at this problem, this paper proposes one improved FCM algorithm, which can be divided into two phases. In the first phase, several intervals will be retrieved based on the histogram of the given image, on which cluster centroids can be computed, and improved FCM will be adopted for image segmentation in the second phase.

2 Concurrent FCM algorithms

As we know, FCM algorithm is an important method for data analysis in pattern recognition and data mining, which has been applied in target tracking and image processing. In essence, FCM-based schema for image segmentation is to replace a hard segmentation with a soft one so as to retain information as much as possible. In conventional FCM, the objective function is minimized iteratively, which can be formalized as follows:

$$J(U,V)=\sum_{i=1}^{C}\sum_{j=1}^{n}u_{ij}^{m}d_{ij}^{2}, \tag{1}$$

where C is the predefined number of clusters, n is the number of pixels in the given image, $m \geqslant 1$ is a parameter to control the fuzziness of the clustering results, u_{ij} is the membership of pixel x_j to the ith cluster such that $\sum_{i=1}^{C}u_{ij}=1$, and $d_{ij}=\|x_j-v_i\|$ is a norm metric, denoting Euclidean distance between pixels and clustering centroids, $v_i=\sum_{j=1}^{n}u_{ij}^{m}x_j/\sum_{j=1}^{n}u_{ij}^{m}$ is the ith cluster centroid. By minimizing the objective function, we can get the membership u_{ij}, which can be used for image segmentation.

Considering that spatial information is not utilized in FCM, Ahmed proposed FCM_S [7], in which the label of one pixel is affected by its neighbor pixels. The objective function in FCM_S is rewritten as

$$J(U,V)=\sum_{i=1}^{C}\sum_{j=1}^{n}u_{ij}^{m}d_{ij}^{2}+\frac{\alpha}{N_R}\sum_{i=1}^{C}\sum_{j=1}^{n}u_{ij}^{m}\sum_{x_k\in N_j}d_{ik}^{2}, \tag{2}$$

where α is a parameter reflecting the preference of neighboring effect, N_j consists of the neighbor pixels of the jth one, N_R is the number of neighbor pixels, and the other symbols are the same as those in FCM. Similarly, the formalization of u_{ij} and v_i of FCM_S can be achieved by minimizing (2).

The procedure of implementing FCM_S is the same as that of FCM, and due to the added neighbor information, FCM_S is more insensitive to noise. However, there are two disadvantages of FCM_S: 1) the efficiency is much lower than FCM due to the second item in the objective function; 2) adding neighbor information makes FCM_S perform poor in convergence. Thus, the predefined number of iterations in FCM_S is usually larger than that in FCM. In order to improve the efficiency further, Szilágyi proposed EnFCM based on the statistical information of the given image. Before performing segmentation, EnFCM will filter the given image I, and the filtered image is denoted by I'. Then, image segmentation is performed on its histogram, in which the objective function is defined as

$$J=\sum_{i=1}^{C}\sum_{j=1}^{q}\gamma_j u_{ij}^{m}(I'(j)-v_i)^2, \tag{3}$$

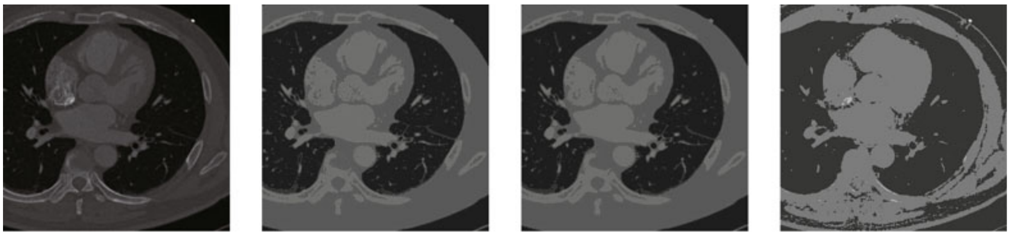

(a) (b) (c) (d)

Figure 1 Comparison of FCM, FCM_S and EnFCM ($C = 4$). (a) A medical image; (b) result of FCM; (c) result of FCM_S; (d) result of EnFCM.

where q is the number of gray levels of the image I', and γ_j is the number of pixels with gray value j. Of course, $\sum_{j=1}^{q} \gamma_j = n$ and $\sum_{i=1}^{C} u_{ij} = 1$. By minimizing the cost function, we will get

$$u_{ij} = \frac{(I'(j) - v_i)^{-2/(m-1)}}{\sum_{k=1}^{C} (I'(j) - v_k)^{-2/(m-1)}}. \tag{4}$$

The most significant advantage of EnFCM is the reduction of running time, because it takes the statistical information into account, which has been overlooked by many FCM-type algorithms [14]. However, EnFCM performs poor when applied in medical image segmentation. For example, the segmentation results of FCM, FCM_S and EnFCM of Figure 1(a) are shown in Figure 1(b), (c) and (d).

As can be seen from Figure 1, the results of FCM and FCM_S are satisfying visually, but they ignore the overall parts of the image. In contrast, the overall difference is detected by EnFCM, which ignores the details instead. From another aspect, the running time of FCM and FCM_S is more than 100 seconds, while that of EnFCM is less than 1 second. Therefore, how to combine the advantages of FCM, FCM_S with EnFCM for image segmentation, is always the focus of many researchers, which is also the starting point of this paper.

3 HisFCM— an improved FCM schema based on histogram

In FCM-type algorithms, though spatial and other information are adopted to get better results and higher efficiency, there still exist several problems, which can be generalized as follows.

1) The cluster is labelled by the cluster centroid, but the centroid does not exist in the given image. Therefore, it will take a long time for all pixels to get close to corresponding cluster centers.

2) Each pixel is dealt with separately in FCM and FCM_S, which may cause such problems: the pixels with equal gray values may have different memberships for one cluster, while those with different gray values may have equal memberships.

For the two above problems, this paper holds the idea that the information in the given image is not fully utilized, and we will illustrate the problem by Figure 2— the histogram of Figure 1(a). As can be seen, if we want to classify the image into four classes with the help of the histogram, we can denote them by four peaks: 10, 58, 67 and 81. Also, we cannot classify pixels with gray value of 11 and pixels with gray value of 68 into one class; otherwise the objective function will not be minimized. In other words, the probability of classifying pixels with gray value of 10 and pixels with gray value of 11 into one class is much higher than that of classifying pixels with gray value of 10 and pixels with gray value of 68 into one class. All of such information is not utilized by FCM-type algorithms, meaning that the information in the given image is not fully mined. Based on this problem, this paper proposes one improved FCM schema based on histogram, which will be denoted as HisFCM in the following sections.

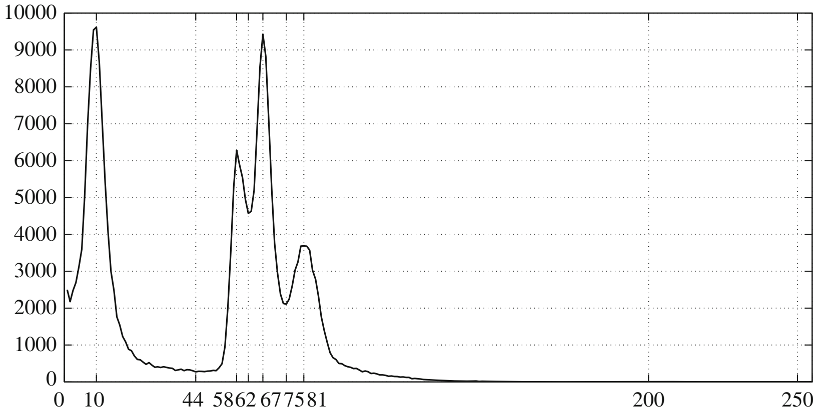

Figure 2 Histogram of Figure 1(a).

The procedure of HisFCM can be divided into two phases: the first is to retrieve C intervals with the help of the histogram, and the second phase will perform image segmentation based on improved FCM algorithm. Over other improved algorithms, HisFCM has the following advantages: 1) with the help of histogram, HisFCM makes the best of the statistical information in the given image, and can have comparable efficiency with EnFCM; 2) the peaks retrieved on the histogram will guide the segmentation in the second phase, which can ensure the effect of segmentation results; 3) cluster centroids are computed based on the intervals retrieved in the first phase, while other algorithms retrieve centroids with the help of all pixels in the image. As a result, HisFCM will improve the efficiency greatly, as will be illustrated elaborately in the following subsections.

3.1 Interval retrieval based on histogram

The idea of retrieving intervals in this paper is inspired by [13], which detected several peaks for image segmentation according to predefined thresholds. Here, after retrieving the peaks, this paper will further construct C intervals. Given the histogram H of an image I, the schema of detecting C peaks proceeds as follows.

Step 1. Find the set P of all peaks in the histogram H, that is, $P = \{i|H(i) > H(i-1), H(i) > H(i+1)\}$.

Step 2. If $\|P\| \leqslant C$, algorithm ends; otherwise goto Step 3.

Step 3. Associate all pixels in the image with the peaks in P according to their gray values, and for each maximum value $i \in P$, compute $N(i)$, the number of associated pixels, formally,

$$N(i) = \|\{j, |I(j) - i| = \arg \min_{k=1..|P|}\{|I(j) - k|\}\}\|. \tag{5}$$

Step 4. Delete the peak i with the least $N(i)$, and re-associate pixels with the rest peaks in P, goto Step 2.

After retrieving the set P, we will construct C intervals based on it. Suppose $P = \{P_1, P_2, \ldots, P_C\}$ such that $P_i < P_{i+1}$ for $i = 1, \ldots, C-1$. Then the ith interval $[l_i, h_i]$ can be retrieved as follows:

1) If $i = 1$, $l_1 = 0$, $h_1 = \arg \min_{P_1 \leqslant i \leqslant P_2}\{H(i)\}$.

2) If $i = C$, $l_C = \arg \min_{P_{C-1} \leqslant i \leqslant P_C}\{H(i)\}$, and $h_C = 255$.

3) Otherwise, $l_i = 1 + \arg \min_{P_{i-1} \leqslant j \leqslant P_i}\{H(j)\}$, and $h_i = \arg \min_{P_i \leqslant j \leqslant P_{i+1}}\{H(j)\}$.

Take the histogram shown in Figure 2 as an example, and suppose $C = 4$. By peak detecting, we will get four peaks: 10, 58, 67 and 81. Based on these peaks, the four constructed intervals are $[0, 44]$, $[45, 62]$, $[63, 75]$ and $[76, 255]$. As we can see, the retrieved peaks are those that can represent the four clusters in our hypothesis, and it is also reasonable to partition the histogram into the four intervals.

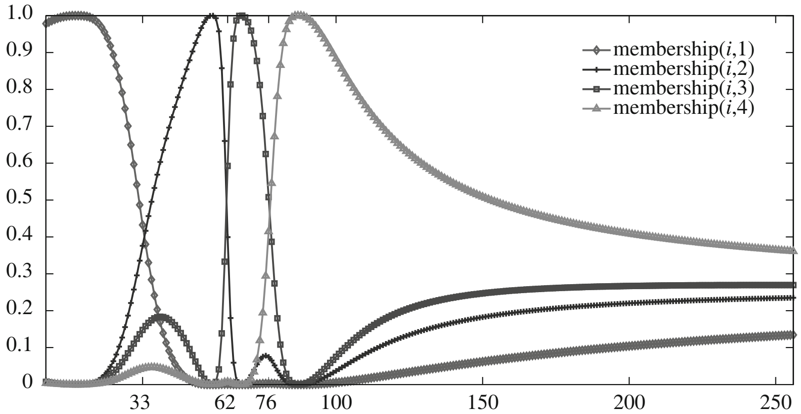

Figure 3 Membership of pixels in Figure 1(a) to corresponding clusters.

3.2 Image segmentation based on improved FCM

This subsection will illustrate the details of applying improved FCM to image segmentation. Based on previous hypothesis, the membership of pixels in $[l_i, h_i]$ to the ith cluster should be larger than that to other clusters, but the pixels with gray values close to l_i and h_i may have comparable membership to two neighbor clusters, which means pixels with gray value near l_i and h_i may belong to other clusters in the final segmentation. In addition, the centroid of the ith cluster should be restricted to be included in $[l_i, h_i]$. Therefore, inspired by EnFCM, the cluster centroids of the improved FCM can be defined as

$$v_i = \sum_{j=l_i}^{h_i} j u_{ij}^m H(j) / \sum_{j=l_i}^{h_i} u_{ij}^m H(j). \tag{6}$$

However, when initializing the algorithm, according to previous hypothesis, the membership of pixels near the centroid should be greater than that of pixels far from the centroid; therefore, the membership cannot be initialized at random. That is to say, the initialized centroids cannot be computed as shown by (6). Instead, for the initial membership of pixels in $[l_i, h_i]$, we will assign 1 to the ith cluster, and 0 to the other clusters. Hence, the cluster centroids can be initialized as follows:

$$v_i = \sum_{j=l_i}^{h_i} j H(j) / \sum_{j=l_i}^{h_i} H(j). \tag{7}$$

Based on the initialized cluster centroids, the improved FCM algorithm in this paper can be implemented as follows.

Step 1. Initialize cluster centroids by (7).

Step 2. Initialize membership u_{ij} by (4), where $i = 1, \dots, C$ and $j = 1, \dots, n$.

Step 3. Compute the objective function J by (3).

Step 4. Update cluster centroids by (6).

Step 5. Update membership u_{ij} by (4).

Step 6. Compute the objective function J' by (3).

Step 7. If $|J' - J| <$threshold, goto Step 8; otherwise let $J = J'$, and goto Step 4.

Step 8. Perform image segmentation based on the membership of pixels to corresponding clusters.

Taking the image in Figure 1(a) as an example, the memberships of pixels retrieved by improved FCM algorithm are shown in Figure 3, in which membership (i, j) denotes the membership of pixel i to jth cluster. As can be seen, pixels near the centroids of corresponding cluster have the maximum membership 1 for this cluster, and 0 for the other clusters. At the same time, we can perform image segmentation based on the membership in Figure 3, where the image is partitioned into four clusters according to the final intervals: [0,33], [34,62], [63,76] and [77,255]. The classes of some pixels in the boundary region of

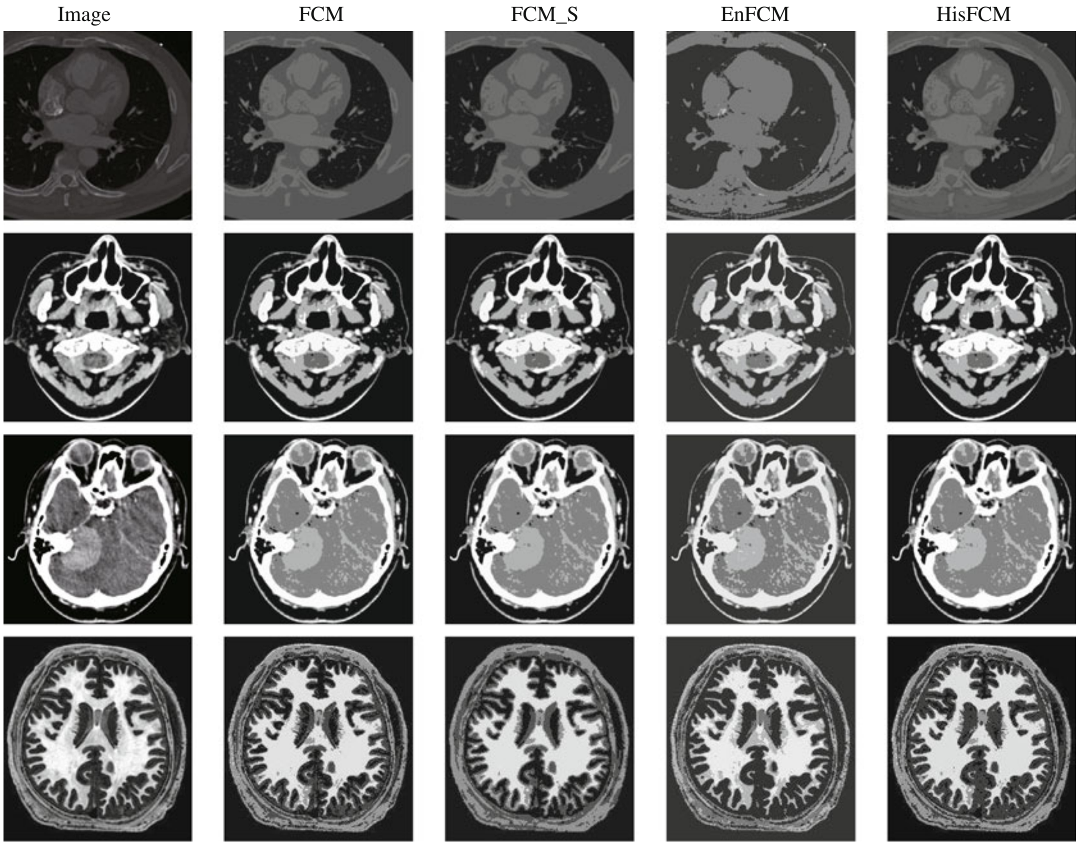

Figure 4 Segmentation results.

initial intervals are different from the intervals retrieved in Subsection 3.1. This is also consistent with previous hypothesis.

The advantage of HisFCM over FCM, FCM_S and other FCM-type algorithms is that it makes the best of the information in the given image, and can improve the efficiency to a great extent. However, different from EnFCM, intervals retrieved in the first phase will guide the procedure of image segmentation, and will restrict the centroids in corresponding intervals, which not only can ensure the satisfying results, but also can improve the efficiency.

4 Experiments

This section will use the medical images in the first column of Figure 4 to illustrate the implementation of HisFCM, and compare HisFCM with FCM, FCM_S and EnFCM from different aspects. We denote the four images simply by breast, head, tumor and brain. The size of breast, head and tumor is 512×512, and the size of brain is 200×217.

4.1 Evaluation of segmentation result

In this subsection, we will compare segmentation results of FCM, FCM_S, EnFCM and HisFCM visually. The parameters in the experiments are set as follows: $C = 4$, threshold$= 0.00001$, $\alpha = 2.0$, $m = 1.75$, and the maximum number of iterations is assigned 100. The segmentation results of the four algorithms are shown in the other four columns of Figure 4. Also, in order to compare the details of the segmentation results, we enlarge the part of the segmentation results, shown in Figure 5.

Figures 4 and 5 show that HisFCM not only performs well for the details of the given images, but also can detect the main difference, which is obvious for image breast in Figure 5. Specifically, segmentation results of breast in Figure 5 show that the main difference cannot be detected by FCM and FCM_S, which

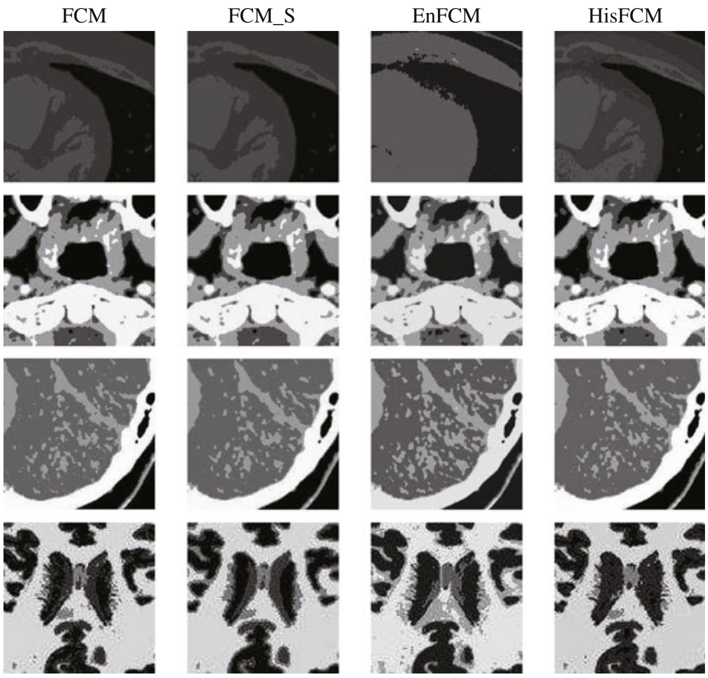

Figure 5 Enlarged part of the results.

is obvious in the results of EnFCM and HisFCM. For other medical images, the details of breast are well distinguished by FCM, FCM_S and HisFCM, yet cannot be well done by EnFCM. As for the segmentation results of head and brain, Figure 5 show that the details and boundaries in the results of FCM, FCM_S and HisFCM are better than those of EnFCM. Also, by incorporating the neighbor information or being guided in segmentation, there are less number of small regions detected by FCM_S and HisFCM, especially in the segmentation results of tumor and head. In summary, HisFCM performs the best, FCM and FCM_S the second and EnFCM performs poor.

4.2 Evaluation of cluster quality

Furthermore, in order to compare the quality of the results quantitatively, we select four measures: Bezdek partition coefficient V_{PC} [16] , V_{XB} proposed by Xie and Beni [17], $F(I)$ proposed by Liu [18] and reconstruct error V_{RE} [19,20], which are specified as follows.

1) Bezdek partition coefficient reflects the biggest memberships of pixels, formalized as follows:

$$V_{\mathrm{PC}} = \sum_{i=1}^{C}\sum_{j=1}^{n} u_{ij}^2. \tag{8}$$

According to the definition of V_{PC}, one good cluster algorithm should make the membership to some cluster as big as possible, but small to other clusters. Therefore, a good cluster algorithm should correspond to V_{PC} of high value.

2) V_{XB} is proposed by Xie and Beni, defined as

$$V_{\mathrm{XB}} = \sum_{i=1}^{C}\sum_{j=1}^{n} \left[u_{ij}^2 I(j) - v_j^2\right] / [n \min_{\forall j\neq k}\{v_j - v_k^2\}]. \tag{9}$$

By (9), the value of V_{XB} reflects the distance between pixels and corresponding cluster centroids in another form. Since we require that pixels of one cluster assemble around the centroid, the algorithm with smaller V_{XB} is preferred.

Table 1 Quality comparison of the four algorithms

Measure	Algorithm	Breast	Head	Tumor	Brain
V_{PC}	FCM	0.908256	0.937925	0.920705	0.860694
	FCM_S	0.890121	0.910757	0.891943	0.753245
	EnFCM	0.780802	0.880398	0.856142	0.872252
	HisFCM	0.889750	0.938482	0.920164	0.867822
V_{XB}	FCM	1.713890	1.528460	1.574370	3.926275
	FCM_S	1.715960	1.529560	1.575089	1.417249
	EnFCM	1.707268	3.361964	1.702101	3.361547
	HisFCM	2.054981	1.525295	1.581734	1.401027
$F(I)$	FCM	0.375072	1.785398	1.611865	6.621822
	FCM_S	0.377370	2.034325	1.777180	9.830825
	EnFCM	3.055097	4.162627	4.451048	7.946504
	HisFCM	0.379563	1.813729	1.647936	6.786621
V_{RE}	FCM	39.986866	96.725337	106.032094	178.802513
	FCM_S	40.237604	105.220361	114.231684	298.485189
	EnFCM	288.016497	630.000703	542.438433	385.641821
	HisFCM	39.124536	103.670048	104.955610	191.218075

3) In [18], Liu designed a criterion for evaluating color image segmentation, called Liu coefficient in this paper. In order to evaluate the segmentation results of gray-scale images, this paper revises Liu coefficient into

$$F(I) = \frac{\sqrt{C}}{n}\sum_{i=1}^{C}\frac{e_i^2}{\sqrt{A_i}}, \tag{10}$$

where A_i is the number of pixels in the ith cluster, $e_i = \sum_{j=1}^{A_i}|I(j) - I'(j)|$, and $I(j)$ and $I'(j)$ are the gray-scale values of the jth pixel in the original and segmented images. From the definition of $F(I)$ in (10), we can conclude that a good cluster algorithm should minimize the difference between the original image and the segmented one, which will result in smaller $F(I)$.

4) Reconstruction error V_{RE} is adopted to measure the distance between reconstructed image and the original one, and the gray values of the reconstructed image can be calculated as follows:

$$I''(i) = \sum_{k=1}^{C} u_{ki}^m I(i) \Big/ \sum_{k=1}^{C} u_{ki}^m. \tag{11}$$

Based on the reconstructed image and the original one, reconstruction error can be expressed in the following form:

$$V_{\mathrm{RE}} = \frac{1}{n}\sum_{i=1}^{n}\|I''(i) - I(i)\|^2. \tag{12}$$

Obviously, we desire that the reconstructed image is approximate to the original image, that is to say, an algorithm with less reconstruction error is thought to be a good one. According to the definitions of the four measures, we compare the four algorithms in our experiments and tabulate the measures in Table 1.

From the Bezdek partition coefficients shown in Table 1, we can see that FCM performs the best in the four algorithms, HisFCM the second, and FCM_S and EnFCM perform poor. From V_{XB}, we can see that HisFCM outperforms the other algorithms except for breast, meaning that pixels in clusters of HisFCM are closer to corresponding centroids, which is consistent with previous hypothesis of this paper. From $F(I)$, we can see that FCM and HisFCM perform well, FCM_S the second, and EnFCM performs poor. As for FCM_S, it is understandable that its $F(I)$ is larger than FCM and HisFCM, for it considers

Table 2 Comparison of running time (s)

Image	FCM	FCM_S	EnFCM	HisFCM
Breast	168.403079	214.454575	0.312002	0.093601
Head	141.648908	414.182655	0.265202	0.062400
Tumor	187.716003	577.266100	0.343202	0.093601
Brain	34.694622	84.848944	0.312002	0.078001

the neighbor information when processing the images. From V_{RE}, FCM and HisFCM perform well in reconstruction error, better than FCM_S and EnFCM.

4.3 Comparison of running time

Except for good visual effect and high cluster quality, one good cluster algorithm must satisfy the real-time requirement of image processing. Hence, the running time of FCM, FCM_S, EnFCM and HisFCM also needs to be compared. It is to be noted that the hard and soft environments are the same for the four algorithms, and they are programmed in MATLAB with the version of R2010b, and the results are shown in Table 2.

As is shown in Table 2, the running time of HisFCM is less than 0.1 s, and can fully satisfy the real-time requirement of image processing. Compared with the other algorithms, the efficiency of HisFCM is higher than that of EnFCM, and far higher than that of FCM and FCM_S.

5 Conclusion

Based on histogram, this paper presents an improved FCM algorithm —HisFCM— which can make the best of information in the given image. Comparatively, HisFCM incorporates the advantages of FCM, FCM_S and EnFCM, and performs well in medical image segmentation. Moreover, the efficiency of HisFCM is much better than that of other improved algorithms, and can meet the real-time requirement of medical processing. However, as a segmentation method only using color information and statistical information provided by the given image, the proposed method may fail in region of interest(ROI) retrieval in images, especially in complex medical images. In future work we will solve this problem with the help of interactive operations.

Acknowledgements

This work was also supported by National Natural Science Foundation of China (Grant Nos. 61020106001, 60933008, 60903109, 61170161), National Science & Technology Pillar Program in the Twelfth Five-year Plan Period (Grant No.2011BAD21B01), Technology Development Programe of Shandong Province (Grant Nos. 2008-GGB01814, 2011GGB01193, 2011GGB01138), Natural Science Foundation of Ludong University (Grant No. LY2010014).

References

1 Chen C, Cheng M, Tan P, et al. Sketch2Photo: Internet image montage. ACM Trac Graph, 2009, 28: 1–8
2 Cheng M, Zhang F, Mitra N, et al. RepFinder: finding approximately repeated scene elements for image editing. ACM Trac Graph, 2010, 29: 1–8
3 Pham D L, Xu C Y, Prince J L. A survey of concurrent methods in medical image segmentation. Annu Rev Biom Eng, 2000, 2: 315–337
4 Ji Z, Sun Q, Xia D. A framework with modified fast FCM for brain MR images segmentation. Patt Recogn, 2011, 44: 999–1013
5 Ji Z, Sun Q, Xia D. A modified possibilistic fuzzy c-means clustering algorithm for bias field estimation and segmentation of brain MR image. Comput Medic Imag Graph, 2011, 35: 383–397

6 Pham D L, Prince J L. An adaptive fuzzy C-means algorithm for image segmentation in the presence of intensity inhomogeneities. Patt Recogn Lett, 1999, 20: 57–68
7 Ahmed M N, Yamany S M, Mohamed N, et al. A modified fuzzy C-mean algorithm for bias field estimation and segmentation of MRI data. IEEE Trans Medic Imag, 2002, 21: 193–199
8 Choi H S, Haynor D R, Kim Y. Partial volume tissue classification of multichannel magnetic resonance images a mixel model. IEEE Trans Medic Imag, 1991, 10: 395–407
9 VanLeemput K, Maes F, Vandermeulen D, et al. A unifying framework for partial volume segmentation of brain MR images. IEEE Trans Medic Imag, 2003, 22: 105–119
10 Szilágyi L, Benyó Z, Szilágyii S M, et al. MR brain image segmentation using an enhanced fuzzy c-means algorithm. In: Proceedings of the IEEE International Conference EMBS, Cancun, 2003. 724–726
11 Chuang K, Tzeng H, Chen S, et al. Fuzzy C-means clustering with spatial information for image segmentation. Comput Medic Imag Graph, 2006, 30: 9–15
12 Wang X, Bu J. A fast and robust image segmentation using FCM with spatial information. Digit Sign Process, 2010, 20: 1173–1182
13 Caldairou B, Passat N, Habas P, et al. A nonlocal fuzzy segmentation method: Application to brain MRI. Patt Recogn, 2011, 44: 1916–1927
14 Cai W, Chen S. Fast and robust fuzzy cmeans clustering algorithms incorporating local information for image segmentation. Patt Recogn, 2007, 20: 825–838
15 Tan K, Isa N. Color image segmentation using histogram thresholding—Fuzzy Cmeans hybrid approach. Patt Recogn, 2011, 44: 1–15
16 Bezdek J C. Cluster validity with fuzzy sets. Cybernet Syst, 1974, 3: 58–73
17 Xie X L, Beni G A. Validity measure for fuzzy clustering. IEEE Trans Pattern Anal Mach Intell, 1991, 13: 841–847
18 Liu J, Yang Y H. Multiresolution color image segmentation. IEEE Trans Patt Anal Mach Intell, 1994, 16: 689–700
19 Pedrycz W. Knowledge-Based Clustering. Hoboken: John Wiley & Sons. 2005
20 Graves D, Pedrycz W. Kernel-based fuzzy clustering and fuzzy clustering: A comparative experimental study. Fuzzy Sets Syst, 2010, 161: 522–543